Fiber coupled waveguide grating structures

Shengfei Feng,[1] Xinping Zhang,[1,a)] Hao Wang,[2] Mudi Xin,[2] and Zhenzhen Lu[2]
[1]*College of Applied Sciences, Beijing University of Technology, Beijing 100124, People's Republic of China*
[2]*College of Materials Science and Engineering, Beijing University of Technology, Beijing 100124, People's Republic of China*

(Received 11 October 2009; accepted 2 February 2010; published online 29 March 2010)

Fabrication and characterization of the miniature device of waveguide grating-structures (WGS) on the end facet of an optical fiber are demonstrated. A layer of ZnO between the fiber and the grating structures serves as the waveguide. The fiber is used to direct the excitation light to the WGS and to carry the signal response back to the detection system. The narrow-band waveguide resonance mode tunable in the visible spectrum can be measured through the fiber in both the transmission and reflection. This nanodevice may be suitable as long-range sensors for the detection of refractive-index changes in nontransparent or toxic liquids. © *2010 American Institute of Physics*. [doi:10.1063/1.3373422]

Waveguide grating-structures (WGS) (Refs. 1–4) exhibit unique physical properties that can be utilized to explore applications in the field of optical filters, optical switches,[5,6] polarizers,[7] and sensors.[8,9] The narrow-band optical response in conjunction with high angle-resolved tunability implies a high sensitivity of this kind of device to the change in the structural and environmental parameters.[10] In particular, using metallic materials to construct the grating structures, one can achieve strong coupling between the waveguide resonance mode and the particle plasmon resonance,[11,12] introducing photophysical mechanisms to be exploited in optoelectronic devices. Sensors are actually the straightforward applications of this kind of nanodevices, where the change in the environmental refractive index induces spectral shifts of both the particle plasmon resonance and the waveguide resonance modes. Usually liquid samples under study have to be circulated or sealed inside a cell where the sensor device is attached. Thus, a sufficient amount of the liquid sample has to be used to fill the cavity inside the cell and to cover the effective area of the nanostructures. Commonly, in a subsequent spectroscopic measurement, a complex optical system is needed and a transmission geometry is preferred due to inconveniences in the measurement on the reflection mode, where both the sensor device and the detection system have to be rotated simultaneously to optimize the spectral position and intensity of the signal. However, the transmission geometry becomes a serious problem in the detection of nontransparent samples.

In this letter, we propose an approach to realize a miniature WGS device as small as 0.28 mm^2 in area on the end facet an optical fiber, exhibiting special functions that cannot be accomplished by the conventional devices fabricated on large pieces of glass substrate (generally $>10\times10$ mm^2 in area and 1 mm in thickness, as illustrated in our previous works[6,7,11]). Thus, the WGS device can be easily employed in some extreme conditions, where there might be very limited space allowed for performing the measurements, the target sample may be difficult to reach, the environmental temperature or pressure might be extremely low or extremely high, the environmental conditions might be hazardous to health, etc. In these cases, the fiber-based WGS device proposed here may show various advantages. Furthermore, the optical spectroscopic measurement system can be significantly simplified through fiber coupling and the nanodevice can be easily integrated into larger optical systems. Some methods for fabricating grating structures on the end facets of fibers have been demonstrated. One- and two-dimensional gratings with a period of 2 μm were inscribed into a polymer thin film on the end facet of a fiber.[13] Gratings with a period of 2 μm have been fabricated on the end facet of a fiber by direct writing using femtosecond laser pulses.[14] Gold gratings with a period of 630 nm were fabricated on the end facet of a fiber using nanoimprint-and-transfer processes.[15] Here, we fabricate nanoscale waveguided photoresist (PR) grating structures using interference lithography on the polished end facet of a fiber with the ZnO waveguide layer deposited using radio-frequency magnetron sputtering. The fiber coupling configuration endows the WGS device with high flexibility particularly in the detection of nontransparent or toxic liquids and for the on-site detection of samples located in confined spaces.

Figure 1(a) shows the photograph of the device based on a fiber-coupled waveguide grating structures (FCWGS) and Fig. 1(b) demonstrates how the waveguide grating structure is arranged on the end facet of the fiber. The PR grating has been fabricated using interference lithography, where the UV light source is produced by a frequency-tripled diode-pumped solid-state laser and the PR S1805 from Rohm and Haas is used as the recording medium. The ZnO waveguide layer was deposited onto to the polished end facet of the fiber using radio-frequency magnetron sputtering and has a thickness of $h=430$ nm. The PR grating has a period of $\Lambda=425$ nm and a modulation depth of about 200 nm. The multimode fiber has a core diameter of 600 μm, a cladding thickness of 10 μm, and a length of about 25 cm. Figure 1(c) demonstrates schematically the basic principle of the waveguide grating device that is coupled with the multimode fiber. The broadband white light is sent into the multimode fiber from the nonstructured end. At the WGS end of the fiber, the propagation modes of the fiber are diffracted by the grating while being reflected by the interfaces and transmitted through the structures. The resonance mode of the WGS is included in the transmitted and reflected beams. The dif-

a)Electronic mail: zhangxinping@bjut.edu.cn.

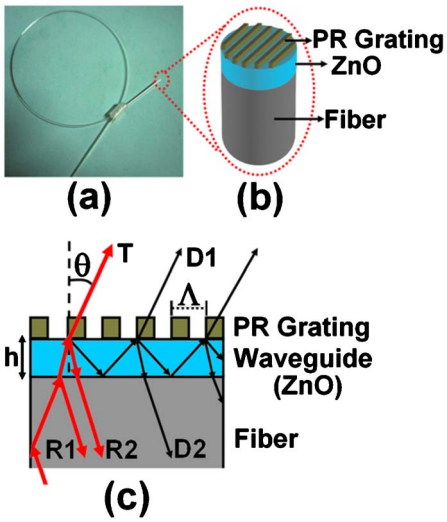

FIG. 1. (Color online) (a) Photograph of the fiber coupled waveguide grating device. (b) Enlarged illustration of the grating structures on the end facet of the fiber. (c) The diffraction geometry for the basic principles of the fiber coupled waveguide grating structures, where R1 and R2 denote the reflection beams, T denotes the transmission beam, and D1 and D2 denote the diffraction beams.

fraction of the fiber modes excites multiple propagation modes in the ZnO waveguide, which induce further diffractions by the grating into the space of the reflected and the transmitted light, respectively, while propagating in ZnO planar waveguide. The diffraction into the space of the transmitted light interferes destructively with the directly transmitted light within a narrow spectral band, which is identified as the resonant mode of the WGS device and is observed as a sharp dip in the transmission spectrum. This corresponds to a narrow-band peak in the reflection spectrum. Because different propagation modes of the fiber have different angles of incidence onto the WGS, multiple resonance modes are excited simultaneously, which correspond to different exit angles of θ as defined in Fig. 1(c). For simplicity, only one fiber propagation mode is sketched in Fig. 1(c). Therefore, at different angles of θ we can measure the resonant waveguide modes corresponding to different incident fiber modes. This enables angle-resolved tuning of the transmission optical response of the device.

Figure 2(a) shows the scanning electron microscopic (SEM) image of a one-dimensional PR grating on the end facet of a fiber. Figure 2(b) shows the diffraction pattern of white light at the WGS end of the fiber, when coupling the white light from a 100 W halogen lamp into the fiber at the unstructured end. The strong diffraction characteristics

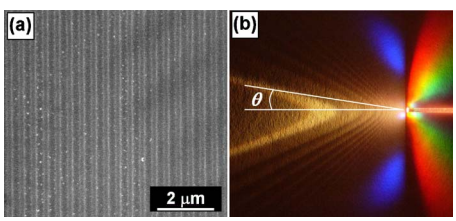

FIG. 2. (Color online) (a) The SEM image of the grating structures on the end facet of the fiber. (b) Photograph of the diffraction pattern at the WGS end of the fiber with the broadband white light coupled into the fiber from the unstructured end.

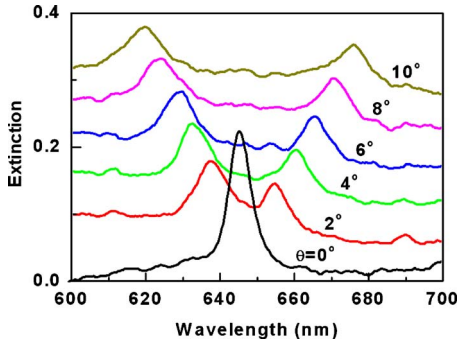

FIG. 3. (Color online) Optical extinction spectra for the transmission resonance mode of the fiber coupled waveguide grating structures as a function of the exit angle (θ).

shown in Fig. 2(b) indicate the excellent quality of the gratings leading to the large modulation depth.

We characterize the optical response of the FCWGS device using the optical extinction spectroscopy, where the optical extinction spectrum is measured as $-\log_{10} T(\lambda, \theta)$, where $T(\lambda, \theta)$ is the transmission of the light through the WGS at a wavelength of λ and at an exit angle of θ with respect to that through the plain fiber without WGS on the end facet. In the measurement, we first determine the orientation of the gratings of WGS using the diffraction pattern as a reference and then optimize the polarization of the incident light to obtain the largest signal in the optical extinction spectrum. A spectrum analyzer USB 4000 from Ocean Optics is used in these measurements.

Figure 3 shows the optical extinction measurements on the FCWGS for the transmission mode over a spectral range from 600 to 700 nm as a function of the exit angle θ, where the polarization of the incident white light has been optimized to obtain the largest signal. At normal incidence, the resonance of the waveguide mode is located at about 645 nm. With increasing the angle θ in the range from 0° to 10° in steps of 2° the extinction peak splits into two branches, which correspond to different propagation modes of the fiber with different incident angles onto the WGS and evolve into opposite directions. The shorter-wavelength branch shifts to about 619 nm and the longer-wavelength one to about 676 nm as θ is increased to 10°, indicating an angle-resolved tuning rate of about 5.7 nm per degree.

The most important advantage of the fiber-coupled waveguide grating device is that it can be used to detect the changes in nontransparent or toxic liquids or other samples that are difficult to reach. Furthermore, the long fiber device enables easy remote detection. The end of the fiber can be extended even into some environments under extreme pressures or at extreme temperatures where conventional measurements fail. In these applications, the reflection mode will be employed, where the resonance mode appears as a pronounced peak in the reflection spectrum.

Considering that the polarization of light may be changed after long-distance propagation through a multimode fiber, which may consequently change the intensity and the spectrum of the resonance signal, we need to characterize the polarization dependence of the reflected resonance signal. The corresponding spectroscopic measurement employs the setup in Fig. 4(a). The white light from a halogen lamp is coupled into the fiber via the unstructured end after passing through the polarizer P_1 and a beam splitter BS.

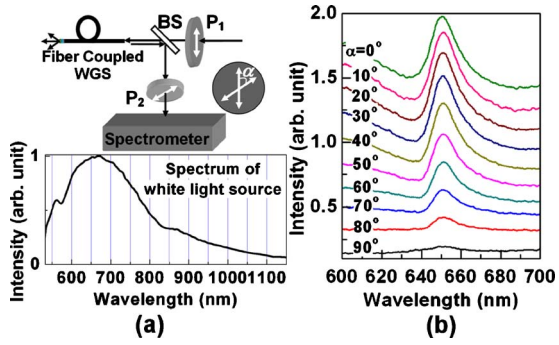

FIG. 4. (Color online) (a) The experimental setup for the measurement of the reflection resonance mode with the spectrum of the white light source given underneath the geometric sketch of the setup. (b) The reflection spectra as a function of the angle (α) between the transmission axes of the polarizers P_1 and P_2.

The reflected light from the fiber that carries the resonance signal is reflected by the BS before passing through the polarizer P_2. The reflection spectrum is then collected at different angles (α) between the transmission axes of P_1 and P_2. The evolution of the reflection spectrum as a function of α is given in Fig. 4(b), where α has been increased from 0° to 90° and the light enters the spectrometer almost along the axis of the detection head of the spectrometer. The transmission axis of P_1 has been first optimized to obtain the maximum resonance signal before the polarizer P_2 is inserted into the light path at the position shown in Fig. 4(a). As can be seen in Fig. 4(b), a strong resonance signal can be detected at a wavelength of about 650 nm and at $\alpha=0$ with a bandwidth of about 14 nm at full width at half maximum. As α is increased to 90°, the resonance signal disappears almost completely, implying that this resonance spectrum is nearly linearly polarized in the same direction as the incident light. This means that the interaction with the WGS and the double-pass propagation through the fiber have very little effect on the polarization of the light. Thus, we can optimize the resonance sensor signal simply by adjusting the polarization of the incident light using P_1 in Fig. 4(a) and the practical optical setup can be thus simplified by leaving out the polarizer P_2. This is important for the practical sensor applications of devices consisting of waveguided gold nanowires, where the light should be polarized perpendicular to the gold nanowires to excite the particle plasmon resonance. However, this kind of polarization dependence may also reduce the signal-to-noise ratio of the sensor signal because the reflection by the unstructured front facet of the fiber and other scattered light will be taken into the measurement data as they have the same polarization as the resonance signal. This needs to be considered in future improvements of the potential sensor scheme. Furthermore, a comparison between the curve at $\theta=0$ in Fig. 4(b) and the spectra in Fig. 3 indicates a small redshift in the resonant signal with a broadened bandwidth. One possible reason is that the axis of the detection fiber of the spectrometer is not exactly along the symmetric axis of the reflected light beam. A more important reason is probably that the reflection resonance mode is actually a superimposition of the interaction of multiple propagation modes in the fiber with the WGS. Different propagation modes in the fiber have been incident onto the WGS at different angles before being reflected back. Thus, the bandwidth of the resonance signal becomes broadened if multiple reflection modes reach and are collected by the detection head of the spectrometer. Actually, one can obtain a narrower signal bandwidth using a larger detection distance of the spectrometer from the unstructured end of the fiber, so that fewer propagation modes from the fiber can be collected by the spectrometer due to the large divergence of the reflected light beam.

In conclusion, we demonstrated a miniature device based on the fiber-based waveguide nanograting structures with narrow-band optical response that is tunable in the visible spectral range. This is potentially suitable for remote sensor applications for the detection of nontransparent or toxic liquids and for the applications in extreme conditions, implying multifold advantages over conventional waveguide grating structures[1] in the development of sensors. Furthermore, a design combining WGS and flexible fibers is important for the construction of filters, optical switches, and other fiber-based optoelectronic devices.

We acknowledge the High-Tech Research and Development Program of China (Grant No. 2007AA03Z306), the Natural Science Foundation of China (Grant No. 10774011), the Project-sponsored by SRF for ROCS, the State Educational Ministry, and the Beijing Educational Commission (Grant No. KZ200810005004) for the financial support, and Professor Peter Klar for very helpful discussions.

[1] D. Rosenblatt, A. Sharon, and A. A. Friesem, IEEE J. Quantum Electron. **33**, 2038 (1997).
[2] R. Magnusson and S. S. Wang, Appl. Phys. Lett. **61**, 1022 (1992).
[3] P. Rochon, A. Natansohn, C. L. Callender, and L. Robitaille, Appl. Phys. Lett. **71**, 1008 (1997).
[4] A. Sharon, D. Rosenblatt, and A. A. Friesem, Appl. Phys. Lett. **69**, 4154 (1996).
[5] D. Nau, R. P. Bertram, K. Buse, T. Zentgraf, J. Kuhl, S. G. Tikhodeev, N. A. Gippius, and H. Giessen, Appl. Phys. B: Lasers Opt. **82**, 543 (2006).
[6] X. P. Zhang, B. Q. Sun, J. M. Hodgkiss, and R. H. Friend, Adv. Mater. (Weinheim, Ger.) **20**, 4455 (2008).
[7] X. P. Zhang, H. M. Liu, J. R. Tian, Y. R. Song, and L. Wang, Nano Lett. **8**, 2653 (2008).
[8] R. Horváth, H. C. Pedersen, N. Skivesen, D. Selmeczi, and B. N. Larsen, Opt. Lett. **28**, 1233 (2003).
[9] G. Nemova and R. Kashyap, J. Lightwave Technol. **25**, 2244 (2007).
[10] S. F. Feng, X. P. Zhang, J. Y. Song, H. M. Liu, and Y. R. Song, Opt. Express **17**, 426 (2009).
[11] X. P. Zhang, B. Q. Sun, R. H. Friend, H. C. Guo, D. Nau, and H. Giessen, Nano Lett. **6**, 651 (2006).
[12] A. Christ, T. Zentgraf, J. Kuhl, S. G. Tikhodeev, N. A. Gippius, and H. Giessen, Phys. Rev. B **70**, 125113 (2004).
[13] S. Choi, K. R. Kim, K. Oh, C. M. Chun, M. J. Kim, S. J. Yoo, and D. Y. Kim, Appl. Phys. Lett. **83**, 1080 (2003).
[14] W. Shin, I. B. Sohn, B. A. Yu, Y. L. Lee, S. C. Choi, Y. C. Noh, J. Lee, and D. K. Ko, IEEE Photonics Technol. Lett. **19**, 550 (2007).
[15] S. Scheerlinck, D. Taillaert, D. Van Thourhout, and R. Baets, Appl. Phys. Lett. **92**, 031104 (2008).